ISSN 1344-3887
RIKEN-AF-AC-30

The Simulation of Emittance growth by Ray-tacing method

C. C. Yun

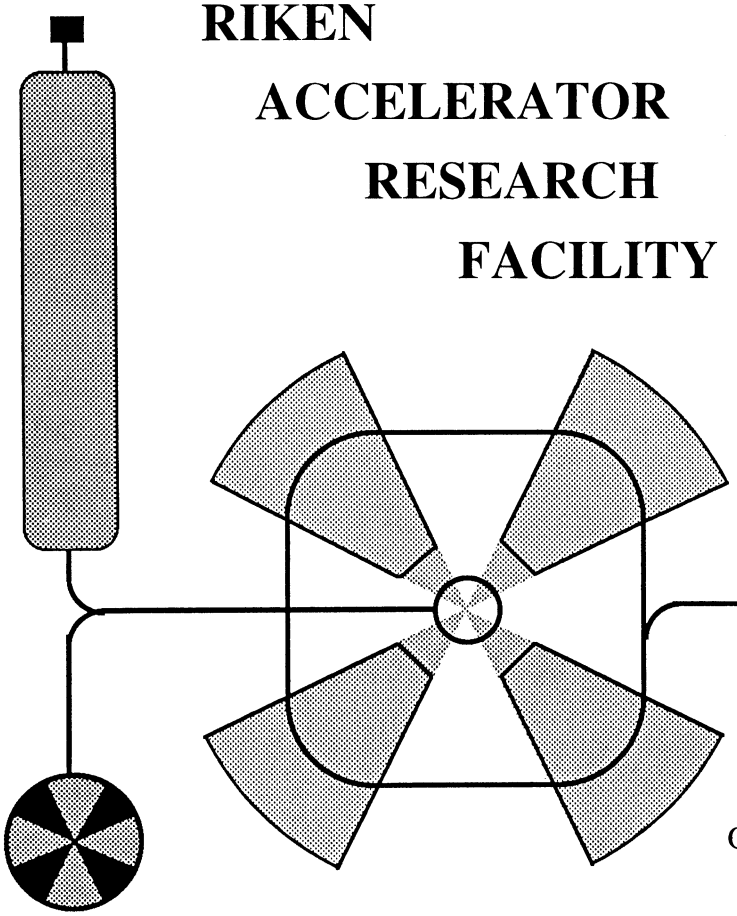

RIKEN
ACCELERATOR
RESEARCH
FACILITY

October 2001

The Institute of Physical and Chemical Research (RIKEN)
2-1 Hirosawa, Wako, Saitama 351-0198, Japan
TEL: (048)462-1111 FAX: (048)462-4642
e-mail: *username*@rikvax.riken.go.jp

The Simulation of Emittance growth by Ray-tacing method

C. C. Yun
RIKEN, Wako-shi, Saitama 351-0198, Japan and

The simulation of emittance growth of RI-beam produced from BigRIPS is performed. The emittance after passing through BigRIPS is roughly 4 times in horizontal and 2 times in vertical larger than the initial emittance.

I. INTRODUCTION

RI-beams produced from projectile fragment separator by the name of BigRIPS are delivered to various experimental setups through beam-delivering system[1]. In addition, BigRIPS provides Accumulator Cooler Ring(ACR) with RI-beams. In the ACR, the beam is cooled by electron cooling and stochastic cooling. Accumulation of the beam is performed by multi-turn injection and RF stacking. The efficient accumulation and cooling of beam depend completely on the production rate, the purity, the momentum spread, and the emittance of RI-Beam. Therefore, RI-beams for injection into ACR should be strongly controlled by constraining factors, namely, the momentum spread of $\Delta p/p = \pm 0.15\%$ and the emittance of $\varepsilon_h = 5\pi mm \cdot mrad$ in horizontal and $\varepsilon_v = 40\pi mm \cdot mrad$ in vertical[2].

The schematic diagram of BirRIPS is shown in Fig. 1. The configuration of BigRIPS can be written as PT-

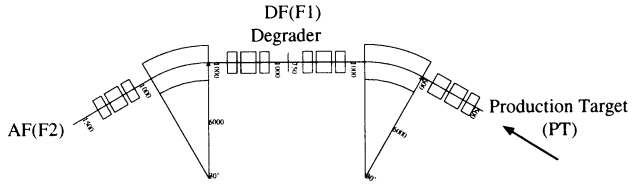

FIG. 1: Schematic view of BigRIPS

TQ-D-TQ-DF(F1)-TQ-D-TQ-AF(F2), whrer PT, TQ, D, DF, and AF represent production target, triplet quadrupole magnets, dipole magnet, dispersive focus point, and acrhomatic focus point, respectively. This system can be divided by two sections. The first section gives a dispersive focus at F1 and analyes the magnetic rigidity of fragment. The second section compensates the dispersion of fisrt section and gives doubly achromatic focus at F2. The wedge-shaped energy degrader is placed at the mid focus point F1. The basic parameters of BigRIPS separator are given in Table I[3]. As seen from Table, BigRIPS has large acceptance and it is unsuitable for ACR in consideration of beam accumulation and cooling time. For injection into ACR, 1.0% in full momentum and $20mrad$ in full angle acceptance are acceptable. However, this momentum spread of $\Delta p/p = \pm 0.5\%$ gives

TABLE I: The basic parameters of BigRIPS separator

	BigRIPS separator
$\Delta\Theta(mrad)$	80
$\Delta\Phi(mrad)$	100
$\Delta p/p(\%)$	7
$(x/x) = F1/F2$	-1.63/1.71
$(x/\delta)(cm/\%)$	-2.36
$(y/y) = F1/F2$	-4.91/1.54
$p/\Delta p$	1450[a]
Max. $B\rho(Tm)$	7.52
$Length(m)$	22.9

[a]First order momentum resolution at mid focus. A beam spot size of $1mm$ is assumed.

rise to the longer cooling time in ACR. In order to eliminate this problem, the momentum spread will be reduced to $\Delta p/p = \pm 0.15\%$ by debuncher cavities located befor ACR[4].

The emittance after passing through BigRIPS is considered. In general, the separation of isotope from the various fragments produced in a production target based on the magnetic rigidity and the energy loss of fragments. The separated fragments passing through degrader have different velocities for different Z, because the energy loss is propotional to Z^2 of the fragment. These fragments are easily separeted by the another dipole magnet and then led to final position. The emittance growth arise from the energy straggling and the multiple scattering of fragment within degrader.

The simulation of emittance of RI-beam produced from BigRIPS was performed. The simulation method and reslut are reported here.

II. SIMULATION METHOD

The simulation was basically carried out by ray-tracing method. This computes the trajectory of particle through a magnetic field and a degrader directly. INTENSTIY[5], Graphic Transport[6] and Graphic Turtle[7] programs were used. In addition, the energy straggling and the multiple scattering of particles within degrager are precisely calculated. The energy loss is determined by Beth-Bloch equation with higher order corrections. The energy straggling is determined

using the method of Tschalär[8]. The multiple scattring is determined using the simple formular from the Particle Data Handbook[9].

The r.m.s emittance can be obtained from

$$\varepsilon = \sigma_x \sigma_{x'} \tag{1}$$

where, σ is the standard deviation. The subscripts of x and x' represent beam extent and beam angle, respectively. σ is given by,

$$\sigma = \sqrt{\frac{1}{N}\sum_{i=1}^{N}(x_i - \bar{x})^2} \tag{2}$$

where $\bar{x}$ is the average of x_i of each point.

The simulation process can be explained to the following.

The information of the variety of fragments, the momentum spread, the scattering angle etc. on the production target are obtained by INTENSITY. Using these information, the particle beam vector which consist of the beam extent, beam angle in horizontal and in vertical, and the momentum spread was created with assumption of Gaussian distribution. The beam extent of $\pm 0.5mm$ is assumed. At the same time, the magnitude of field of each magnet of BigRIPS was determied to reproduce the transfer matrix in Table I with Transport program. The aspect of beams passing through BigRIPS were simulated with Turtle program.

The simulation falls into three stages.

- Firstly, from PT to F1(before degrader)
- Secondly, within degrader
- Thirdly, from F1(after degrader) to F2

The particle vectors of the beams at ecah stage were written into files. The r.m.s emittance at PT, F1(before and after degrader), and F2 was calculated.

III. SIMULATION RESULT

Figure 2 shows the simulation results of ^{55}Ni without degrader at production target(PT) and at achromatic focus(F2). In this simulation, the number of particles was 2000. The top and bottom in Fig. 2 represent the emittance at PT and F2, respectively. The left and right in figure indicate horizontal and vertical, respectively. The information of ^{55}Ni is shown in Table II, which is the example output of INTENSITY. The primary beam of ^{58}Ni with $1p\mu A$ and the production target, ^{9}Be, of $1850mg/cm^2$ were assumed. The fragments in Table very close to magnetic rigidity of ^{55}Ni and would be main contaminants coming with ^{55}Ni beam in ACR[10]. As seen from Fig. 2, the emittance at F2 differ slighly from initial emittance at PT. The difference comes from the effect of non-linear terms of BigRIPS. The small increase in the emittance is count for nothing considering the emittance growth by the degrader.

TABLE II: Example output of INTENSITY for ^{55}Ni

Fragment (Charge)	Momentum (MeV/c)	$\Delta p/p$ (%)	Angle (mrad)
$^{51}Fe(26^+)$	39274.2	0.58	7.27
$^{53}Co(27^+)$	40761.5	0.49	6.51
$^{55}Ni(28^+)$	42244.5	0.46	5.73
$^{56}Ni(28^+)$	43111.0	0.34	5.31

Figure 3 shows the simulation results for the main beam of ^{55}Ni and contaminants of ^{51}Fe, ^{53}Co, and ^{56}Ni, at PT and at F1 just before degrader. For this simulation, the number of each particle was 2000. The top figures show that all RI-beams huddle together at production target. The bottom figures show that ^{56}Ni beam was separated by magnetic rigidity at F1. Unseparated RI-beams, ^{51}Fe and ^{53}Co, should be separated by degrader.

Figure 4 shows the result at F1 after passing through degrader with $d/R = 0.3$ and at F2. The energy of ^{55}Ni beam was about $220MeV/u$ at this time. The top figures indicate the results including the effect of degrader, namely, the energy staraggling and the multiple scattering. The bottom figures show that ^{51}Fe and ^{53}Co beams were clearly separated.

Figure 5 shows the simulation results with momentum slit and postition slit. The momentum slit of $\pm 0.5\%$ was located just after the degrader and the position slit of $\pm 1cm$ located at F2. The top figures with only momentum slit and the bottome with momentume and position slit are presented. As seen from Fig. 5, the main contami-

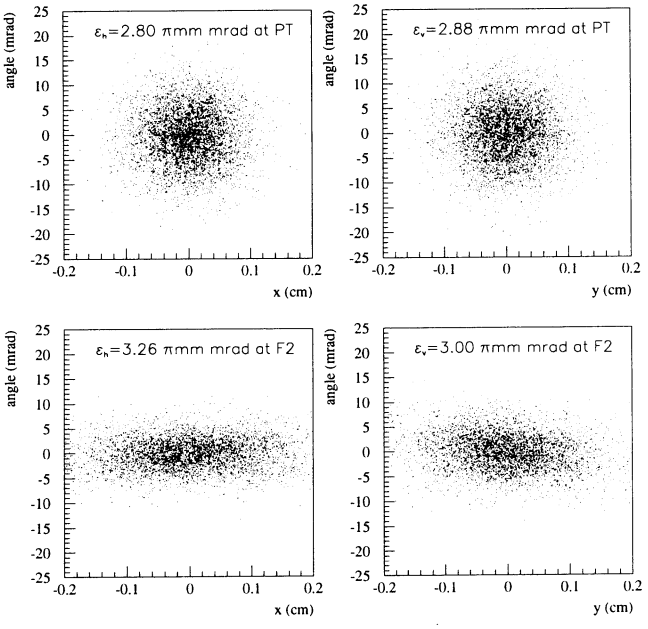

FIG. 2: The simulation result without degrader for ^{55}Ni

nants, ^{51}Fe, ^{53}Co, and ^{56}Ni were reduced by momentum slit and position slit.

The process of RI-beam production, take ^{55}Ni for example, was shown by now. In fact, how the emittance growth arising from the energy straggling and the multiple scattering within degrader are shown in Fig. 6.
The top figures are the emittance at PT and the bottom figures are the emittacne at F2. The horizontal emittance of $2.90\pi mm \cdot mrad$ at PT change into $10.94\pi mm \cdot mrad$ at F2. The vertical emittance of $2.85\pi mm \cdot mrad$ at PT change into $6.49\pi mm \cdot mrad$ at F2. The horizontal emittance at F2 is roughly 4 times larger than initial emittance at PT. In the case of verical, the emittance is roughly 2 times larger than initial emittance.
The same results applied to ^{106}Sn. In the same manner as ^{55}Ni, to obtain ^{106}Sn beam of $220MeV/u$ with the degrader $d/R = 0.3$ determined the produciton target thickness. The same results are obtainable for avaiable RI-Beams, as long as the degrader of $d/R = 0.3$ is used.

For the result above, the main reason why the large emittance growth in horizontal compared with in vertical is that the energy straggling and the multiple scattering contribute to the emittance growth in horizontal, however only the multiple scattering contribute to emittance growth in vertical[5](see also APPENDIX A). As mentioned earlier, the emittance of RI-beam for injection into ACR is required to be $\varepsilon_h = 5\pi mm \cdot mrad$ in horizontal and $\varepsilon_v = 40\pi mm \cdot mrad$ in vertical. However, the emittance growth is predominant in horizontal than

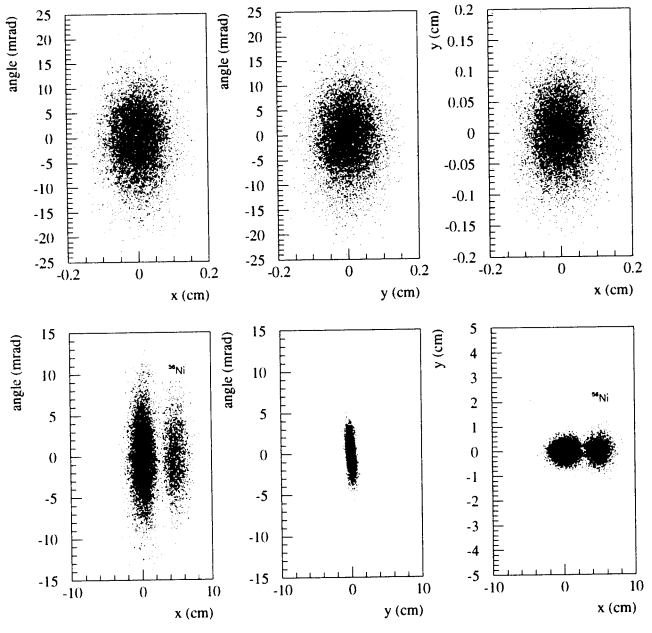

FIG. 3: The simulation result with degrader for ^{55}Ni and contaminants at PT(top) and at F1 just before degrader(bottom). Left, center, and right in figure indicate horizontal emittance, vertical emittance, and postion, respectively.

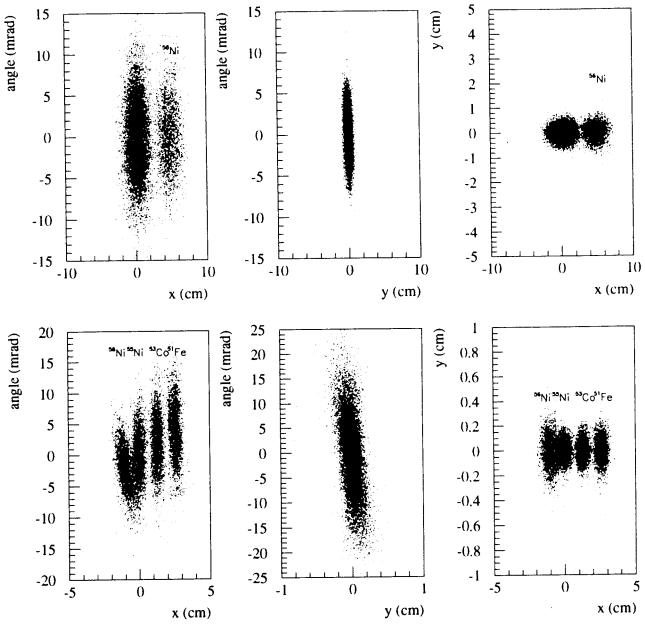

FIG. 4: The simulation result with degrader of $d/R = 0.3$ for ^{55}Ni and contaminants at F1 after degrader(top) and at F2(bottom). Left, center, and right in figure indicate horizontal emittance, vertical emittance, and postion, respectively.

in vertical. Therefore, horizontal-vertical rotation device should be installed at beam line before the injection point of the ACR to transfer the emittance from horizontal to vertical. This rotation device would be Skew Q which consist of nothing less than 4 quadropole magnets[11]. The simulation result with Skew Q can not be shown by insufficient investigation for the present.

IV. SUMMARY

The simulation of emittance growth of ^{55}Ni beam was carried out by ray-tracing method. The information of fragments were obtained from INTENSITY program. The aspect of particles passing through BigRIPS was simulated with Turtle program.

The emittace in horizontal was roughly 4 times larger than the initial emittance. In the case of vertical, the emittance was roughly 2 times larger than the initial emittance.

As briefly mentioned earlier, although the emittance growth is inevitable because of degrader, horizontal-vertical rotation device such as Skew Q would come up for the one of solutions of RI-beam with the emittacne growth for injection into ACR. For the Skew Q, it needs futher consideration.

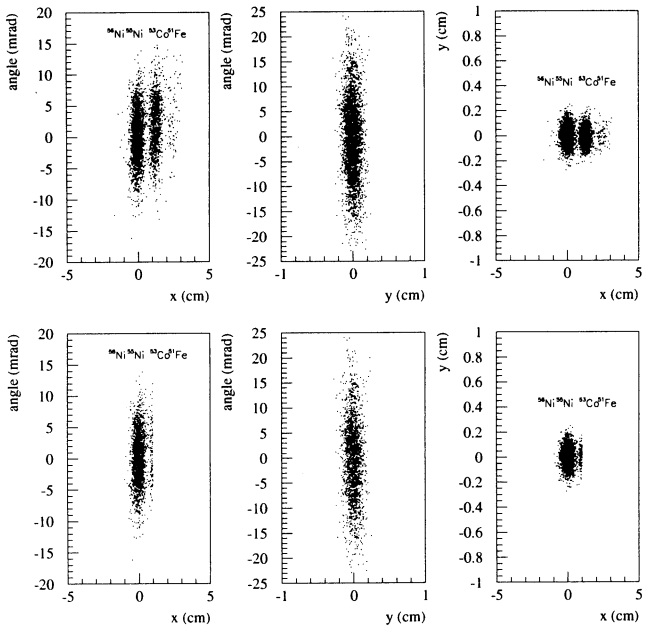

FIG. 5: The simulation results with momentum slit of $\pm 0.5\%$ located just after the degrader(top) and position slit of $\pm 1.0cm$ located at F2(bottom)

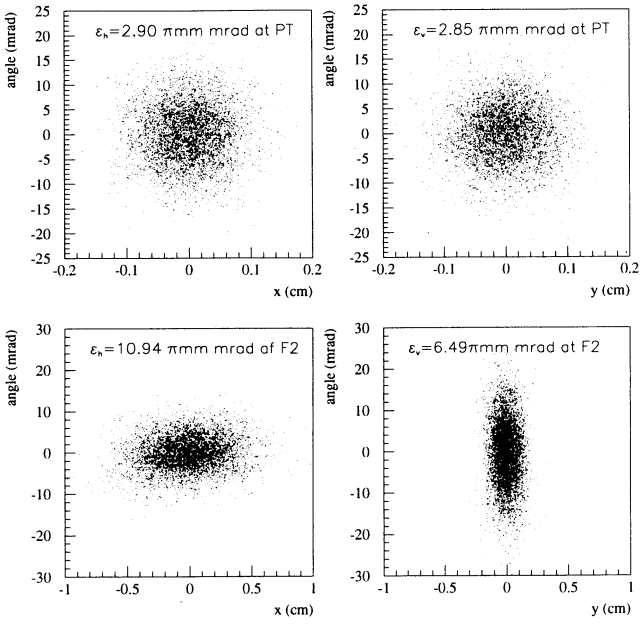

FIG. 6: The emittance for ^{55}Ni at PT(top) and at F2(bottom)

ACKNOWLEDGMENTS

I greatefully acknowledge helpful discussion with Dr. M. Takanaka on several points in the paper. I wish thank Dr. N. Inabe for helpful suggestion and comments. Special thanks are due to Dr. K. Kusaka for providing me with the information of BigRIPS.

REFERENCES

[1] Y. Yano et al., Proc. of PAC2001, ROPA007
[2] MUSES Conceptual Design Report, p.93, November 2000
[3] K. kusaka, private communication
[4] MUSES Conceptual Design Report, p.74, November 2000
[5] J.A. Winger, B.M. Sherill and D.J. Morrissey, Nucl. Instr. Meth., B**70** 380 (1992)
[6] PSI Graphic Transport Framework by U. Rohrer based on a CERN-SLAC-FERMILAB version by K.L. Brown et al., Transport, a Computer Program for Designing Charged Particle Beam Transport System, CERN 73-16 (1973) and CERN 80-04 (1980)
[7] PSI Graphic Turtle Framework by U. Rohrer based on a CERN-SLAC-FERMILAB version by K.L. Brown et al., Decay Turtle, CERN 74-2 (1974)
[8] C. Tschaläar, Nucl. Instr. Meth., **64** 237 (1968)
[9] Particle Data Group (eds.), Review of Particle Properties, Phys. Lett. B**239** 1 (1990)
[10] MUSES Conceptual Design Report, p.82, November 2000
[11] N. Inabe, private communication

APPENDIX A: THE EMITTANCE USING TRANSFER MATRIX

The emittance including the effect of degrader can be written by tranfer matrices. The transfer matrices for the BigRIPS are, repectively,

$$R1 = \begin{pmatrix} M_{1x} & 0 & 0 & 0 & D_{1x} \\ 0 & \frac{1}{M_{1x}} & 0 & 0 & 0 \\ 0 & 0 & M_{1y} & 0 & 0 \\ 0 & 0 & 0 & \frac{1}{M_{1y}} & 0 \\ 0 & 0 & 0 & 0 & 1 \end{pmatrix} \quad \text{(A1)}$$

for the first section from procution target to dispersive image, F1,

$$R2 = \begin{pmatrix} M_{2x} & 0 & 0 & 0 & D_{2x} \\ 0 & \frac{1}{M_{2x}} & 0 & 0 & 0 \\ 0 & 0 & M_{2y} & 0 & 0 \\ 0 & 0 & 0 & \frac{1}{M_{2y}} & 0 \\ 0 & 0 & 0 & 0 & 1 \end{pmatrix} \quad \text{(A2)}$$

for the second section from the F1 to final image, F2,

$$W = \begin{pmatrix} 1 & 0 & 0 & 0 & 0 \\ 0 & 1 & 0 & 0 & 0 \\ 0 & 0 & 1 & 0 & 0 \\ 0 & 0 & 0 & 1 & 0 \\ W_x & 0 & 0 & 0 & W_\delta \end{pmatrix} \quad \text{(A3)}$$

for the degrading wedge. In these matrices, $M_{ij}(D_{ij})$ refer to the magnification(dispersion) of the jth dimension in the ith section, and W_x and W_δ refer to the effect the degrading material has on the x and δ dimensions. W_x include the information of wedge angle of degrader as well. For a doubly achromatic system, second section matrix $R2$ using $R1$ and the magnification of from production target to F2, M_x and M_y is given by

$$R2 = \begin{pmatrix} \frac{M_x}{M_{1x}} & 0 & 0 & 0 & -\frac{M_x}{M_{1x}}D_{1x} \\ 0 & \frac{M_{1x}}{M_x} & 0 & 0 & 0 \\ 0 & 0 & \frac{M_y}{M_{1y}} & 0 & 0 \\ 0 & 0 & 0 & \frac{M_{1y}}{M_y} & 0 \\ 0 & 0 & 0 & 0 & 1 \end{pmatrix} \quad \text{(A4)}$$

To obtain the final image size(X_3) and angle($X_3^{'}$), apply W and R2(Eq. A4) to R1. X_3 and $X_3^{'}$ get,

$$X_3 = M_x X_0(1 - D_{1x}Wx) + \frac{Mx}{M_{1x}}D_{1x}\delta_0(1 - D_{1x}W_x - W_\delta) - \frac{Mx}{M_{1x}}D_{1x}\delta_w \quad \text{(A5)}$$

$$X_3^{'} = \frac{1}{M_x}X_0^{'} + \frac{M_{1x}}{M_x}\Delta\theta_{ms}/\sqrt{2}, \quad \text{(A6)}$$

where X_0 and $X_0^{'}$ is initial beam spot size and angle, respectively. δ_w and $\Delta\theta_{ms}$ is the energy straggling and the multiple scattering within degrader, repectively. The multiple scattering is converted space into plane by use of factor $\sqrt{2}$.

With the assumption of the Gaussian ditribution describing the fragmentation, Eq. A5 and Eq. A6 can be written as

$$\sigma_{X_3}^2 = M_x^2\sigma_{X_0}^2(1 - D_{1x}W_x)^2 + \left(\frac{M_x}{M_{1x}}\right)^2 D_{1x}^2\sigma_{\delta_0}^2(1 - D_{1x}W_x - W_\delta)^2 - \left(\frac{M_x}{M_{1x}}\right)^2 D_{1x}^2\sigma_{\delta_w}^2 \quad \text{(A7)}$$

$$\sigma_{X_3^{'}}^2 = \left(\frac{1}{M_x}\right)^2\sigma_{X_0^{'}}^2 + \left(\frac{M_{1x}}{M_x}\right)^2\sigma_{\Delta\theta_{ms}}^2/2 \quad \text{(A8)}$$

where,

$$\sigma_{\delta_w} = \frac{100\sigma_{E_w}}{A_f m_0 \beta_2^2\gamma_2^2} \quad \text{(A9)}$$

where, A_f is fragment mass, m_0 is the unified atomic mass, β_2 and γ_2 refer to the beam after the degrader. The energy straggling, σ_{E_w} in a degrader is determined using the method of Tschaläar[8].

$$\sigma^2(E_f) = \left[\frac{dE}{dx}(E_f)\right]^2 \int_{E_f}^{E_i} \frac{d\sigma^2(E)/dx}{[dE/dx(E)]^3}dE \quad \text{(A10)}$$

where, dE/dx is the energy loss. It is determined by Beth-Bloch equation with higher order correction.
The multiple scattering is determined by

$$\sigma(\theta) = \frac{14.1MeV/c}{\sqrt{p_i\beta_i p_f\beta_f}}Z_i\sqrt{\Delta x/L_r}[1 + \frac{1}{9}\log\frac{\Delta x}{L_r}]. \quad \text{(A11)}$$

where the angular width is given in terms of radiation length, L_r, and the initial and final momenta, p_i and p_f, and velocities, $\beta_i c$ and $\beta_f c$.

The degrader with a wedge shape is used to preserve the achromatism of the system. So that, the second term of X_3 and σ_{X_3} in Eq. A5 and Eq. A7 is negligible. Eq. A5 and A7 can be written as,

$$X_3 = M_x X_0 W_\delta - \frac{M_x}{M_{1x}}D_{1x}\delta_w \quad \text{(A12)}$$

$$\sigma_{X_3}^2 = M_x^2\sigma_{X_0}^2 W_\delta^2 - \left(\frac{Mx}{M_{1x}}\right)^2 D_{1x}^2\sigma_{\delta_w}^2 \quad \text{(A13)}$$

With above equations, the horizontal emittance including the effect of degrader can be written,

$$\varepsilon_h = \sqrt{M_x^2\sigma_{X_0}^2 W_\delta^2 - \left(\frac{M_x}{M_{1x}}\right)^2 D_{1x}^2\sigma_{\delta_w}^2}\sqrt{\left(\frac{1}{M_x}\right)^2\sigma_{X_0^{'}}^2 + \left(\frac{M_{1x}}{M_x}\right)^2\sigma_{\Delta\theta_{ms}}^2/2} \quad \text{(A14)}$$

$$\varepsilon_h = \sqrt{\sigma_{X_0}^2 W_\delta^2 - \left(\frac{1}{M_{1x}}\right)^2 D_{1x}^2\sigma_{\delta_w}^2}\sqrt{\sigma_{X_0^{'}}^2 + M_{1x}^2\sigma_{\Delta\theta_{ms}}^2/2} \quad \text{(A15)}$$

The vertical emittance using initial beam size, Y_0, and

angle, $Y_0^{'}$ is obtained by,

$$\varepsilon_v = \sqrt{\sigma_{Y_0}^2}\sqrt{\sigma_{Y_0^{'}}^2 + M_{1y}^2\sigma_{\Delta\theta_{ms}}^2/2} \tag{A16}$$

From Eq. A15 and Eq. A16, it is obvious that the energy straggling and the mutliple scattering within degrader contribute to the emittace growth in horizontal and the only multiple scattering contribute to the emittance growth in vertical.